Geochemistry and solute fluxes of volcano-hydrothermal systems of Shiashkotan, Kuril Islands

Elena Kalacheva [a], Yuri Taran [b,*], Tatiana Kotenko [a]

[a] *Institute of Volcanology and Seismology, Russian Academy of Sciences, Petropavlovsk-Kamchatsky 683006, Russia*
[b] *Institute of Geophysics, Universidad Nacional Autónoma de México, Coyoacán, México D.F., 04510, Mexico*

A B S T R A C T

Shiashkotan Island belongs to the Northern Kuril island arc and consists of two joined volcanoes, Sinarka and Kuntomintar, with about 18 km of distance between the summits. Both volcanoes are active, with historic eruptions, and both emit fumarolic gases. Sinarka volcano is degassing through the extrusive dome with inaccessible strong and hot (>400 °C) fumaroles. A large fumarolic field of the Kuntomintar volcano situated in a wide eroded caldera-like crater hosts many fumarolic vents with temperatures from boiling point to 480 °C. Both volcanoes are characterized by intense hydrothermal activity discharging acid SO_4-Cl waters, which are drained to the Sea of Okhotsk by streams. At least 4 groups of near-neutral Na-Mg-Ca-Cl-SO_4 springs with temperatures in the range of 50–80 °C are located at the sea level, within tide zones and discharge slightly altered diluted seawater. Volcanic gas of Kuntomintar as well as all types of hydrothermal manifestations of both volcanoes were collected and analyzed for major and trace elements and water isotopes. Volcanic gases are typical for arc volcanoes with $^3He/^4He$ corrected for air contamination up to 6.4 R_a ($R_a = 1.4 \times 10^{-6}$, the air ratio) and $\delta^{13}C$ (CO_2) within −10‰ to −8 ‰ VPDB. Using a saturation indices approach it is shown that acid volcanic waters are formed at a shallow level, whereas waters of the coastal springs are partially equilibrated with rocks at ~180 °C. Trace element distribution and concentrations and the total REE depend on the water type, acidity and Al + Fe concentration. The REE pattern for acidic waters is unusual but similar to that found in some acidic crater lake waters. The total hydrothermal discharge of Cl and S from the island associated with volcanic activity is estimated at ca. 20 t/d and 40 t/d, respectively, based on the measurements of flow rates of the draining streams and their chemistry. The chemical erosion of the island by surface and thermal waters is estimated at 27 and 140 ton/km²/year, respectively, which is 2–3 times lower than chemical erosion of tropical volcanic islands.

© 2015 Published by Elsevier B.V.

1. Introduction

The total flux of components degassed from magmas through persistently degassing volcanoes comprises the volcanic vapor flux from fumaroles to the atmosphere, the diffuse flux through volcanic slopes, the hydrothermal flux to the local hydrologic network and components retained in hydrothermal reaction products. The hydrothermal flux from a volcano-hydrothermal system may arise from the discharge of fluids formed at depth over the magma body and/or by acid waters which are formed by the absorption of the ascending volcanic vapor by shallow ground water (Giggenbach et al., 1990; Hedenquist et al., 1994; Rowe et al., 1995; Giggenbach, 1996; Taran and Peiffer, 2009, among others). The part of the anion composition (mainly Cl and SO_4) of the discharging thermal waters from a volcano-hydrothermal system that originates from the volcanic vapor should be taken into account in estimations of the magmatic volatile output and volatile recycling in subduction zones (Hedenquist et al, 1994; Taran, 2009; Shinohara, 2013). Another important application of the hydrothermal solute fluxes from volcanoes is a knowledge about the amount of the leached rock that is estimated from the cation components and silica in the discharging thermal waters. The rate of the leaching (chemical erosion) is directly related to the stability of volcanic edifices (Lopez and Williams, 1993; Reid et al., 2001) and also plays an important role in the chemical balance of the ocean (Rad et al., 2007 and references therein). The metal volcano-hydrothermal flux also has implications for ore-forming processes (Hedenquist et al., 1994).

Here we report the chemical (major and trace elements) and isotopic composition of acidic and neutral thermal waters, chemical and isotopic composition of volcanic vapors and solute fluxes from Shiashkotan Island in the northern part of the Kuril chain (Fig. 1 a, b). Shiashkotan is a remote and hardly accessible island, and little is known about its volcanological settings. Stratula (1969) and Markhinin and Stratula (1977) were the first to describe the hydrothermal activity of the island. The island consists of two active volcanoes, Sinarka and Kuntomintar, both with strong and hot fumaroles, and both are characterized by intense hydrothermal activity in the form of
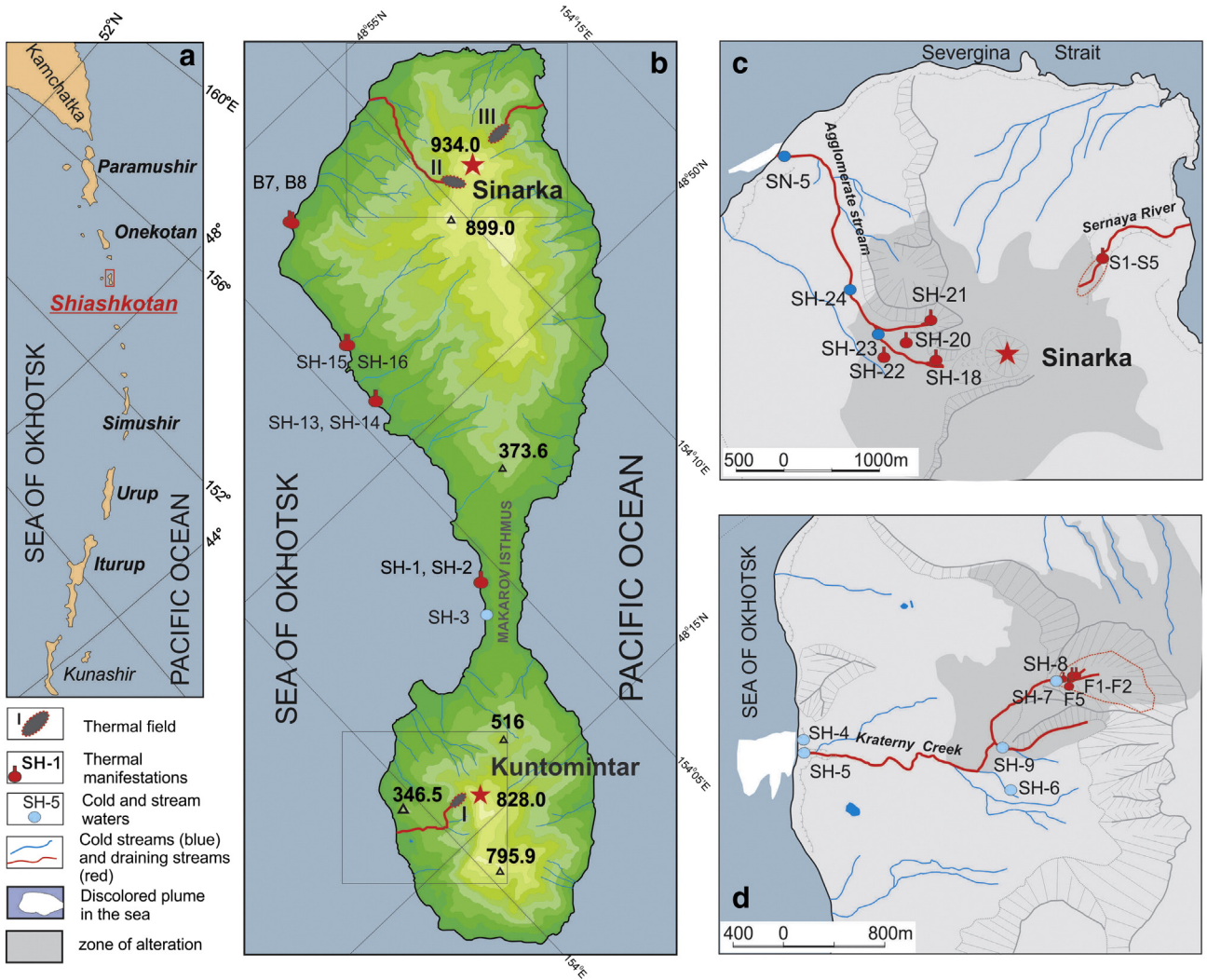
Fig. 1. Shiashkotan Island, Kurils. (a) Shiashkotan position within the Kuril island arc; (b) thermal fields and coastal springs of the island; (c) thermal fields of Sinarka volcano. Numbers of points correspond to numbers in Table 1. (d) Thermal field and samples of Kuntomintar volcano.

Fig. 2. The lava dome and fumaroles of Sinarka volcano. Photo by Elena Kalacheva.

Fig. 3. The summit part of Kuntomintar volcano. Photo by Tatiana Kotenko.

numerous hot and cold springs of acidic SO_4-Cl waters at relatively high levels at highly altered slopes of both volcanoes. Thermal fields discharging acidic waters are drained by streams into the Sea of Okhotsk. There are also 4 groups of hot neutral springs with high Cl content, which are located near the sea level, within tide zones, on the Sea of Okhotsk coast and one small seep on the Pacific coast at the base of Kuntomintar. Hot fumarolic vents of the Sinarka extrusive dome were inaccessible during the 2011 season. Zharkov et al. (2011) have measured ~450 °C in one of the dome fumaroles of Sinarka in 2008. We found a 480 °C fumarole in the active crater of Kuntomintar.

In this paper, we discuss our own (collected during the field campaign in 2011) and all existing data (Markhinin and Stratula, 1977; Taran, 1992; Zharkov et al., 2011) on the geochemistry of volcano-hydrothermal fluids of Shiashkotan. We present data on major and trace element (including REE) chemistry in all types of waters of the island, water isotopic composition of main thermal manifestations and chemical and isotopic composition of volcanic gases of Kuntomintar.

Using the chemistry and flow rates of the main hydrothermal drainage streams, we calculate the total hydrothermal flux of magmatic Cl and SO_4 from the island. We also estimate the total solute discharge that is provided by two main fluxes: the runoff of cold surface water and by subsurface waters with a high contribution of thermal waters. The calculated weathering dissolved flux for Shiashkotan is compared with the chemical erosion of tropical volcanic island (Rad et al., 2007).

2. Volcanology, hydrogeology and thermal manifestations

Shiashkotan Island is a part of the Kuril-Kamchatka subduction zone and is located close to the middle of the entire, almost 2000 km-long, volcanic arc. The island extends from SW to NE for 26 km and has an area of 118 km² (Fig. 1). It has a dumb-bell form with a narrow (~1 km) Makarov Isthmus in the middle. Sinarka volcano (Fig. 2, 910 m asl) composes the northern part of the island and Kuntomintar (Fig. 3, 809 m asl)—the southern part. The distance between summits

Table 1
Coordinates and field data on thermal and cold waters of Shiashkotan Island sampled in 2011.

Sample site	N°	N	E	Z, m asl	T, °C	pH$_{field}$	Eh, мB	S, μS/cm	Q, L/s
Kuntomintar volcano									
Fumarolic condensate	SH11	48°45′32.22″	154° 0′46.16″	390		2.3	310	10080	
Kraterny stream, source 1	SH7	48°45′32.29″	154° 0′47.02″	389	18.4	2.42	265	6580	4
Thermal spring	SH8	48°45′33.51″	154° 0′43.70″	364	64.5	2.35	311	3370	0.3
Kraterny stream, source 2	SH9	48°45′27.89″	154° 0′18.33″	253	21.1	2.99	234	3790	7
Cold spring	SH4	48°45′55.14″	153°59′16.90″	2	9.5	3.8	179	2110	5
Kraterny mouth	SH5	48°45′53.43″	153°59′14.47″	1	9.4	3.46	198	1463	500
Sinarka volcano, North-West Field									
Thermań spring	SH18	48°52′29.44″	154°10′13.66″	538	51.2	2.67	279	8040	7
Thermal spring	SH20	48°52′40.13″	154°10′6.87″	480	37.6	3.21	234	4610	5
Thermal spring	SH22	48°52′41.30″	154°10′0.39″	462	42.6	3.00	271	5750	4.5
Agglomerate stream	SH23	48°52′44.87″	154°10′0.65″	417	21.3	3.38	211	3180	15
Coastal hot springs									
Zakatnye	SH1	48°47′38.64″	154° 4′32.45″	1	53.4	6.03	52	12600	0.1
Zakatnye	SH2	48°47′34.09″	154° 4′24.21″	0.5	30.0	5.94	63	8310	0.2
Vodopadnye	SH15	48°51′42.57″	154° 5′58.74″	1	55.6	6.88	9	12850	0.2
Vodopadnye	SH16	48°51′42.54″	154° 5′58.92″	1	63.8	6.3	47	12660	0.1
Drobnye	SH13	48°50′46.05″	154° 5′34.32″	0.5	43.0	6.27	47	18260	0.2
Drobnye	SH14	48°50′45.64″	154° 5′34.39″	0.5	43.4	6.66	21	17760	0.1
Cold waters									
Makarov stream	SH3	48°46′48.92″	154° 2′35.65″	1	5.6	7.66	-36	101	100
Rain	R	48°46′48.19″	154° 2′19.77″		5.0		124	38	
Rock samples									
Stream-bed sediments	RK	Close to SH8		360					
	RS	Close to SH18		530					

Table 2
Gas composition (mmol/mol) of fumaroles of Kuntomintar volcano and of bubbling gas from Zakatnye springs. Water isotopes in permil vs V-SMOW and $\delta^{13}C$ in permil vs V-PDB. Air is extracted from analyses. In Zakatnye springs the gas contained ~3.4 vol% of O_2 in both samples.

Sample	Date	T, °C	H_2O	H_2	CO_2	CO	Stot	HCl	N_2	Ar	He, ppm	He/Ne	δD, ‰	$\delta^{18}O$, ‰	R/R_a, Corr.	$\delta^{13}C$-CO_2, ‰
F1	07.1987	155	935	0.26	45.6	0.000	17.2	0.98	0.85	0.013	0.32	0.79	−39	−0.9	6.4	−10.2
F2	07.1987	166	964	0.018	23.1	0.000	7.78	0.25	3.09	0.072	0.18	1.3	−44	−2.9	5.3	−8.7
F5	06.2011	480	981	0.006	15.5	5.8E−5	3.20	0.083	0.34	0.004	0.52					
F5	06.2011	480	984	0.0005	12.8	5.0E−6	2.85	0.064	0.27	0.004	0.45		−38	−0.3		
Zakatnye	07.1987	71.2		0.000	870	0.000	0.00	0.00	129	0.77	1.6	1.4			4.8	−7.8
Zakatnye*	06.2011	53		0.000	891	0.000	0.00	0.00	108	1.11	nd		−58	−7.7		

*) In this sample CH_4 was also determined at 0.57 mmol/mol and hydrocarbons with $CH_4/C_{2+} = 35$, where C_{2+} is the total concentration of hydrocarbons with carbon number ≥ 2.

Table 3
Some important ratios of gas components and calculated fractions of the volatiles from mantle (M), sediments (S) and limestone (L). See text for explanations.

Sample	$CO_2/^3He$	$Cl/^3He$	N_2/Ar	N_2/He	M	S	L
F1	1.6×10^{10}	3.4×10^8	65	2656	0.75	0.24	0.01
F2	1.7×10^{10}	1.8×10^8	43	17166	0.64	0.26	0.10
F5			85				
F5			68				
Zakatnye	0.8×10^{10}		97	92142	0.60	0.23	0.17

of Sinarka and Kuntomintar is ~18 km. According to Gorshkov (1970) and Stratula (1969), Sinarka is a complex stratovolcano of the Somma-Vesuvius type with the remains of at least two explosive craters, old caldera walls and a young actively degassing extrusive dome since 1878 (Gorshkov, 1970). Kuntomintar reveals remains of several Holocene explosive craters at the summit part. The hydrothermally active crater of Kuntomintar is a large amphitheater opened to the west, the eroded former crater of the direct blast with highly altered crater walls (Stratula, 1969; Gorshkov, 1970). The last eruption occurred in 1872 (Gorshkov, 1970; Markhinin and Stratula, 1977). Both volcanoes are composed of basaltic to andesitic lava flows and pyroclastics. The youngest active extrusive dome of Sinarka (Fig. 2) is composed of andesite (Stratula, 1969).

According to the Atlas (2007), the average annual precipitation at this part of the Kuril Islands is ~1300 mm. This means that the hydrological balance of the island is maintained by the surface flows (runoff) and infiltration with a total discharge of ~5 m³/s and a negligible evaporation because of a low annual temperature (~ + 4 °C). The surface water table is represented by small lakes, springs, perennial snow and marshy areas. Makarovsky stream (SH-3, Fig. 1), with a source in a canyon with perennial snow, and located relatively far from thermal fields of Kuntomintar, is a typical representative of fresh surface waters of the island.

There are two main thermal fields at Sinarka (Fig. 1b, c). One is located to the west of the extrusive dome at altitudes 350–500 m asl and consists of several separated thermal grounds. According to Markhinin and Stratula (1977), in 1964 there were at least 6 thermal grounds in the main somma-crater at the contact with the extrusive dome. We found 3 small thermal fields (Fig. 1) with numerous small spring discharges having temperatures of 37–52 °C, the field pH of 2.6–3.2 and conductivities from 4.1 to 8.04 mS. Thermal waters from grounds 1–3 are drained by the Agglomeratovy stream to the Severgin Strait between Shiashkotan and Kharimkotan islands. The NE thermal field of Sinarka is described by Markhinin and Stratula (1977) and also by Zharkov et al. (2011). This is a large (500 × 700 m²) field with boiling-point steam vents at the upper part and numerous small hot pools and hot springs at lower levels. Stratula (1969) estimated the total discharge of diluted near-neutral sulfate-bicarbonate-chloride waters with the total salinity < 1.5 g/L and Ca as the main cation as ~20 l/s. This field is drained by the Sernaya (Sulfur) river to the Pacific Ocean (Fig. 1c).

Thermal manifestations of Kuntomintar are situated in the Central and NE craters of the volcano (Fig. 1b, d). In the Central crater, there
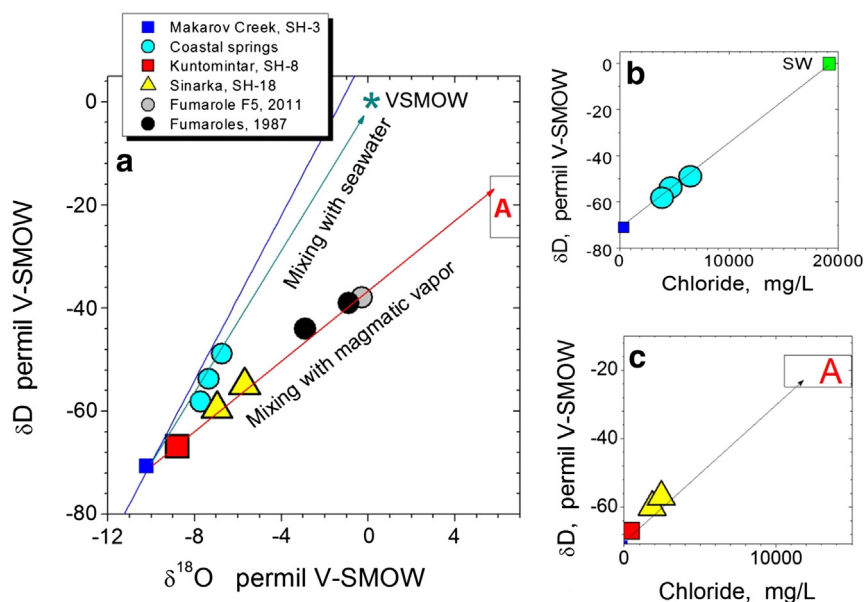

Fig. 4. Isotopic composition of volcanic gas condensates, thermal and cold waters of Shiashkotan. Rectangle A denotes isotopic composition of arc magmatic waters. See text for more details.

Table 4
Chemical (mg/l) and isotopic (‰ VSMOW) composition of thermal and cold waters of Shiashkotan Island.

Sample site	N°	Year	T, °C	pH$_{lab}$	Eh mV	SiO$_2$	B	TDS g/L	Cl⁻	HCO$_3^-$	SO$_4^{2-}$	Na⁺	K⁺	Ca²⁺	Mg²⁺	Al³⁺	Fe³⁺	δD	δ¹⁸O	Ref.
Kuntomintar volcano																				
Upper Kraterny stream 1	SH7	2011	18.4	2.4	265	123	0.4	5.41	312	0	3826	64	2.0	413	27	356	195			1
Thermal spring	SH8	2011	64.5	2.4	311	314	2.0	5.43	462	0	3463	64	2.0	365	29	338	181	−67	−8.8	1
Upper Kraterny stream 2	SH9	2011	21.1	2.6	234	165	2.0	4.03	185	0	2787	50	2.0	297	22	260	147			1
Cold spring	SH4	2011	9.5	3.6	179	110	<0.28	1.87	67	0	1258	64	2.0	108	103	93	0.05			1
Kraterny mouth	SH5	2011	9.4	2.9	198	67	0.4	1.11	67	0	730	23	1.4	98	8.8	63	2.2			1
Thermal spring	K1	1964	78	1.9	na	16	na	5.6	609	0	3738	128		396	73.8	531	117			2
Thermal spring	K2	1970	67	2.5	390	210	na	7.09	794	0	3659	1404	16	321	24.3	75	262			2
Upper Kraterny stream 1	K3	1970	17	2.5	445	236	6.0	7.37	687	0	3950	7.8	5	576	157	476	212			2
Sinarka volcano, North-East Field																				
Geyserny spring	S1	1964	78.0	7.6	na	147	0.9	1.09	69	154	406	100	9.0	122	26	na	0.5			2
Burlyaschy spring	S2	1964	90.0	3.0	na	113	0.7	0.83	42	0	380	87		72	18	na	2.0			2
Thermal spring	S3	1964	59.0	6.8	na	147	1.2	0.69	27	147	165	40		67	19	na				2
Thermal spring	S4	1964	25.0	4.6	na	65	1.7	1.49	96	1.8	709	105	5.6	174	50	na				2
Black Dragon spring	S5	2007	93.1	7.1	na	92	na	1.34	20	92	580	84	12.0	217	47	na	0.1			3
Sinarka volcano, North-West Field																				
Thermal spring	SH18	2011	51.2	2.7	279	283	8.8	6.20	2538	0	1538	385	30	545	501	49	106			1
Thermal spring	SH20	2011	37.6	3.2	234	196	4.7	4.15	1065	0	1727	160	10.6	513	238	744	14			1
Thermal spring	SH22	2011	42.6	3.0	271	182	4.0	4.74	1384	0	1827	250	21.2	489	338	44	68	−60	−7.0	1
Thermal spring	SN1	1964	25.0	4.6	na	75	1.3	1.49	95	1.8	709	105	5.6	174	50	na	na			2
Thermal spring	SN2	2007	38.1	2.8	na	158	na	4.29	1028	0	1960	175	11.2	536	304	na	90			3
Thermal spring	SN3	1964	65	3.3	na	130	6.7	8.98	2633	0	3593	2539	91	350	201	na	na			2
Thermal spring	SN4	1964	45	2.3	na	20	15	3.28	642	0	1794	216	20	329	154	137	na			2
Agglomerate stream	SH23	2011	21.3	3.4	211	111	2.6	2.29	682	0	845	112	4.1	272	136	29	12			1
Agglomerate stream (mouth)	SN5	1964		3.5		113		2.85	359	0	1625	328		426	84	na	30			2
Coastal hot springs																				
Zakatnye	SH1	2011	53.4	6.0	52	74	4.9	7.64	3834	338	474	2399	195	80	170	<0.3	<0.05	−58	−7.7	1
Zakatnye	SH2	2011	30.0	5.9	63	69	0.1	3.06	1420	290	182	839	36	150	33	<0.3	<0.05			1
Zakatnye	B1	1970	58	6.3	310	67	15.2	8.94	6909	427	771	4010	60	346	304	na	na			2
Zakatnye	B2	1964	43	6.8	na	114	4.8	5.54	2661	207	519	1475	80	370	55	na	na			2
Vodopadnye	SH15	2011	55.6	6.9	9	167	11.7	8.84	4658	112	711	2450	114	240	220	<0.3	<0.05	−54	−7.3	1
Vodopadnye	SH16	2011	63.8	6.3	47	167	11.3	8.69	4587	129	584	2433	120	260	246	<0.3	<0.05			1
Vodopadnye	B3	1964	87	6.6	na	198	16	15.79	8520	146	926	4976	100	359	355	na	na			2
Drobnye	SH13	2011	43.0	6.3	47	125	7.6	12.88	6780	226	1058	3730	211	240	394	<0.3	<0.05	−48	−6.7	1
Drobnye	SH14	2011	43.4	6.7	21	136	7.6	12.43	6461	209	1003	3639	257	240	355	<0.3	<0.05			1
Drobnye	B4	1962	71	6.4	na	162	13.5	14.47	7957	149	990	4789		284	32	na	na			2
Drobnye	B5	1962	79	6.4	na	135	9.6	11.80	6351	126	813	3589	173	195	339	na	na			2
Drobnye	B6	1964	60	7.0	na	176	5.3	13.30	7100	226	957	3886	96	288	462	na	na			2
Bashmachnye	B7	1965	74.0	6.6	na	155	na	4.35	2304	106	109	1247	70	245	8.1	na	na			2
Bashmachnye	B8	1962	71.0	6.4	na	216	na	7.20	3816	81	355	2273		249	91	na	na			3
Cold waters																				
Makarov stream	SH3	2011	5.6	7.1	−36	11.5	<0.28	0.08	14.2	17.1	13.4	8.3	0.4	8.4	1.5	<0.3	<0.05	−71	−10.2	1
Makarov stream	MS	1970	na	7.2	170	na	na	0.16	25	61	30	29		14.4	4.1	na	na			2
Vodopadny stream	VS	1964	na	5.4	na	0.3	na	0.27	29	2.4	128	28		32	8.3	na	na			2
Cold spring	CS	1964	na	6.9	na	17	na	0.21	43	26	60	18		28	8.4	na	na			2
Rain	R	2011	na	4.5	124	0.6	<0.28	0.01	2.1	0	6.2	1.3	2.3	0.8	<0.12	<0.3	<0.05			1
Rain2	R1	1964	na	5.5	na	0.3	na	0.07	30	12.2	8	15		na	6.7	na	na			2

References: 1—this work; 2—Markhinin and Stratula (1977); 3—Zharkov et al. (2011).
na—not analyzed.

are several tens of strong fumaroles, some of them with sulfur cones and temperatures <160 °C. The highest temperature fumarole (F5) is located at the northern part of the Central crater at ~400 m asl. Two inaccessible fumarolic vents were found in the NE crater that is open to the north and continues as a deep canyon with a stream that enters into the Sea of Okhotsk. Thermal springs in the Central crater are distributed along the Craterny Creek between 300 and 400 m asl, the main runoff way from the western slope of the volcano and the main drainage of thermal waters. Markhinin and Stratula (1977) have mentioned about ~20 small springs with ultra-acid (pH 1.5–1.9) water and maximal temperature of 80 °C observed in 1963–1964. In 2011, we found numerous hot seeps along the creek and a spring with temperature of 65 °C, flow rate of 0.5 l/s and field pH of 2.16.

Along the western coast of the island 6 groups of near-neutral hot springs with relatively high salinity have been reported by Stratula (1969) and Markhinin and Stratula (1977). These authors estimated the total visible outflow rate of these coastal springs as ~50 l/s. We found and have sampled only 3 groups: (Vodopadnye, Drobnye and Zakatnye, Fig. 1b). All these springs are situated within the low tide zone and associated with contacts between dikes or lava flows with pyroclastics or alluvium. Coordinates, temperatures and flow rates (if measured) of all thermal manifestations of Shiashkotan are shown in Table 1.

Alteration zones within thermal fields with discharging fumaroles and acid SO$_4$-Cl waters are similar to other well-described crater zones like Vulcano (e.g., Fulignati et al., 1999) or Satsuma Iwojima (Hedenquist et al., 1994). It is mainly silicic alteration within fumarolic
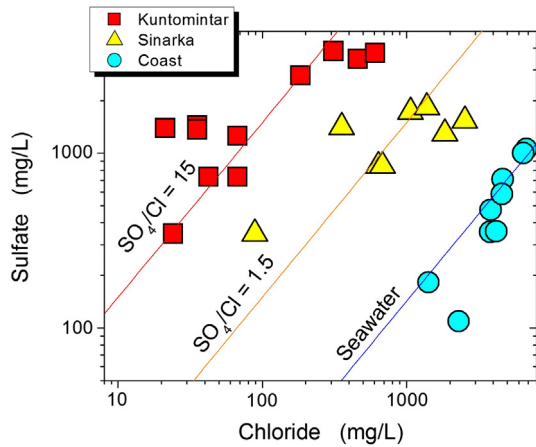
Fig. 5. Chloride-sulfate systematics of thermal waters of Shiashkotan. For coastal springs, Cl/SO$_4$ is close to the seawater ratio. Acid volcanic waters from Kuntamintar and Sinarka form separate clusters with different average Cl/SO$_2$ and with Sinarka waters are more chloride-rich.

fields, the result of almost complete leaching by ultra-acid fluids. These zones are surrounded by large areas of the advanced argillic alteration with alunite, sometimes covered by gypsum and jarosite and large spots of precipitated iron oxides along dry streambeds. We took samples of the streambed sediments: one from Kuntomintar thermal field and one from the NW field of Sinarka for comparing their trace element abundances with the composition of volcanic acid waters.

3. Methods

Volcanic gas samples were taken using a Ti sampling tube and Giggenbach bottles filled with 4 N NaOH solution. Condensates of volcanic vapor were collected using bubblers cooled with snow. Simultaneously with collection of the condensate, samples of dry gas were taken in two-valve gas ampoules. Bubbling gas from Zakatnye springs was taken using a funnel into 15 ml glass tubes with septum. Gas samples from Giggenbach bottles were analyzed following Giggenbach and Goguel (1989). Carbon of CO$_2$ and He isotopes were analyzed from samples of dry gas using procedures described in Rozhkov and Verkhovsky (1990). Condensate samples were used for determining water isotopes.

Water samples were collected in plastic bottles after filtration through a 0.45 μm MILLIPORE. Temperature (± 0.1 °C), pH (± 0.05 units) and conductivity (± 2 %) were measured in situ by an Orion multimeter. Samples for cations analyses were acidified with ultra-pure nitric acid. Concentrations of major dissolved species (Na, K, Ca, Mg, Cl, SO$_4$) were determined using wet chemistry methods and atomic absorption spectroscopy (AAS) in the Institute of Volcanlogy and Seismology, Kamchatka. Alkalinity as HCO$_3^-$ was measured by titration using a 0.1 M HCl solution. Total SiO$_2$ by colorimetric method using ammonium molybdate (Giggenbach and Goguel, 1989). The analytical errors are usually less than 5%.

Trace element concentrations were determined by ICP-MS (Agilent 7500 CE). All determinations were performed with the external standard calibration method, using Re and In as internal standards. The accuracy of the results (5 to 10%) was obtained by analyzing certified reference materials (NRCSLR-4, SPS-SW1 and NIST-1643e).
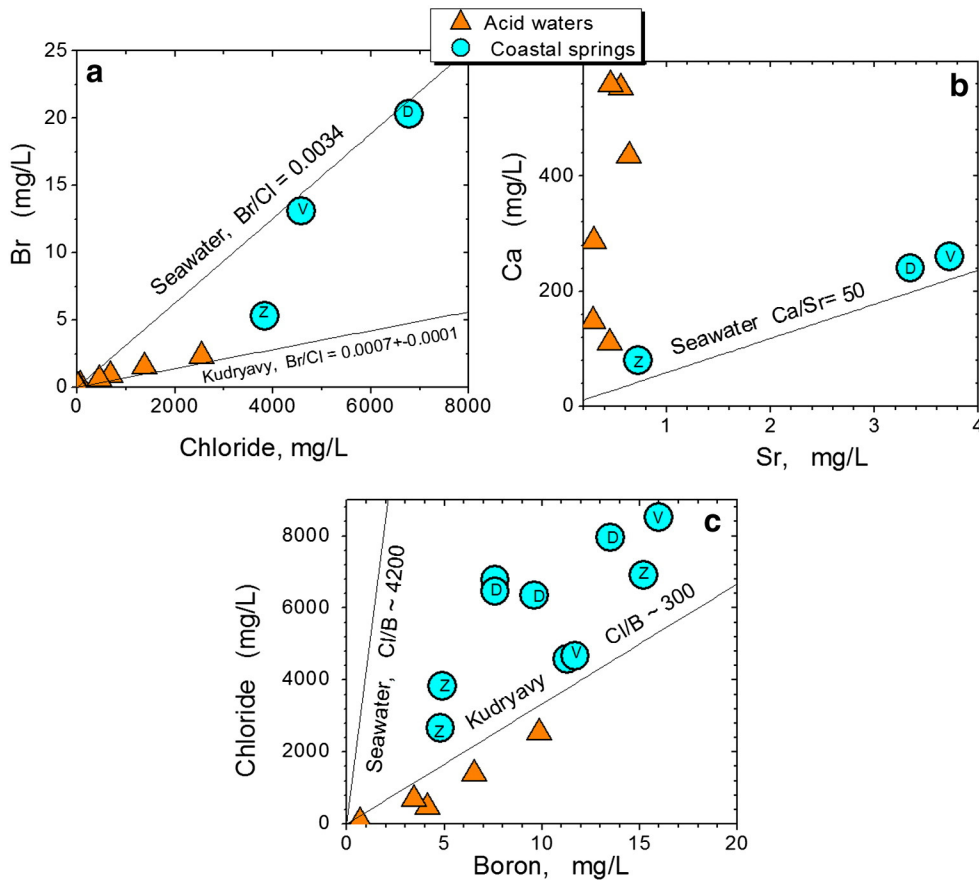

Fig. 6. (a) Br vs Cl plot for thermal waters of Shiashkotan. Also is shown seawater mixing line and a correlation found for Kudrtavy volcano from the same Kuril arc (Taran et al., 1995; Wahrenberger et al., 2002). (b) Ca vs Sr plot shows points for coastal springs close to seawater mixing line and no correlation for volcanic acid waters. (c) Chloride vs Boron correlations. Boron concentrations are between seawater line and a correlation found for Kudrtavy volcano from the same Kuril arc (Taran et al., 1995; Wahrenberger et al., 2002). Labels for coastal springs: D—Drobnye; V—Vodopadnye; Z—Zakatnye.

Table 5
Trace elements in thermal waters of Shiashkotan.
Concentrations in μg/L; bd—below detection limit. REE and Y are highlighted by bold Italic font.

Element	SHK 5	SHK 8	SHK 11	SHK 1	SHK 13	SHK 16	SHK 18	SHK 22	SHK 23	Detection
pH	*3.46*	*2.16*	*1.70*	*6.03*	*6.27*	*6.30*	*2.67*	*3.00*	*3.18*	**Limit, ppb**
t, °C	*9*	*65*	*480*	*53*	*43*	*64*	*51*	*43*	*21*	
TDS, g/L	*0.5*	*5.4*	*1.3*	*7.7*	*12.9*	*8.7*	*5.2*	*3.6*	*1.8*	
Li	10.2	42	7.3	211	556	812	151	121	64	0.25
Be	0.87	5.3	0.021	0.014	0.028	0.054	1.05	0.80	0.59	0.01
B	685	4134	16290	3726	9150	12303	9850	6537	3445	0.29
Al	77910	486320	1344	471	75	76	30913	11878	29297	4.8
P	87	646	123	514	63	99	57	83	55	1.7
Sc	7.0	57	0.059	0.065	0.050	0.041	8.2	3.91	5.3	0.0009
Ti	4.09	35	313	8.8	1.95	1.26	2.11	3.79	11.2	0.094
V	14.7	290	0.72	1.96	0.72	0.29	0.40	17	9.5	0.007
Cr	17	9.0	12.5	8.5	15	13.5	17	17	17	0.026
Mn	1823	4018	51	35	1518	1341	36659	23265	11616	0.16
Fe	32602	215196	412	1732	511	1789	113930	166704	62364	1.90
Co	22	19	1.15	0.40	1.35	0.12	11.5	1.73	5.4	0.003
Ni	10.6	6.6	29	5.5	6.8	6.1	9.5	8.5	9.8	0.20
Cu	11.6	1.05	1.71	2.57	23	2.6	29	2.03	12.3	0.20
Zn	136	633	4335	16	90	9.0	537	458	246	1.53
Ga	1.22	6.6	0.088	0.14	0.35	0.31	2.90	1.83	1.08	0.002
Ge	0.23	3.50	0.057	0.93	7.5	9.9	0.72	0.69	0.36	0.01
As	22	337	2.55	82	656	1446	2.96	54	10.8	0.07
Se	0.74	6.4	6.7	9.2	23	13.5	6.9	8.1	1.91	0.06
Br	137	583	1033	5317	20347	13063	2261	1461	865	0.61
Rb	4.33	25	1.12	47	186	237	156	103	54	0.02
Sr	287	637	452	722	3725	3345	553	459	297	0.11
Y	*22*	*98*	*0.60*	*0.27*	*bd*	*bd*	*19*	*29*	*18*	*0.05*
Zr	0.68	0.39	0.66	0.40	0.39	0.43	0.58	0.56	0.86	0.004
Nb	0.025	0.042	0.020	0.016	0.023	0.024	0.042	0.031	0.025	0.0004
Mo	0.35	0.32	0.30	6.0	11.6	4.55	1.58	1.20	0.79	0.006
Ag	0.49	0.20	1.84	0.34	0.44	0.40	0.54	0.59	0.58	0.004
Cd	0.39	1.19	18	0.14	0.17	0.056	0.84	0.45	0.42	0.007
Sn	0.74	0.42	2.78	0.42	0.56	0.44	0.62	0.95	0.80	0.016
Sb	0.043	0.040	0.93	0.14	2.97	29	0.052	0.080	0.051	0.002
Cs	0.17	1.37	0.12	5.1	50	123	29	11.3	6.5	0.000
Ba	8.1	20	19	29	115	191	37	11.2	18	0.16
La	*2.23*	*11.7*	*0.36*	*0.10*	*bd*	*0.0058*	*1.43*	*1.21*	*1.35*	*0.020*
Ce	*7.5*	*36*	*0.37*	*0.22*	*0.0057*	*0.0047*	*4.17*	*5.9*	*5.0*	*0.005*
Pr	*1.52*	*7.2*	*0.19*	*0.062*	*bd*	*bd*	*0.67*	*1.34*	*1.00*	*0.016*
Nd	*9.0*	*40*	*0.30*	*0.10*	*0.040*	*0.052*	*4.66*	*9.4*	*6.5*	*0.005*
Sm	*3.05*	*13.8*	*0.041*	*0.023*	*0.0073*	*0.0048*	*1.82*	*4.23*	*2.51*	*0.001*
Eu	*1.02*	*5.1*	*bd*	*0.11*	*bd*	*bd*	*0.71*	*1.38*	*0.90*	*0.033*
Gd	*3.95*	*16*	*0.042*	*0.022*	*bd*	*bd*	*2.85*	*5.9*	*3.39*	*0.006*
Tb	*0.70*	*3.24*	*bd*	*0.042*	*bd*	*bd*	*0.52*	*0.99*	*0.61*	*0.013*
Dy	*4.34*	*21*	*0.060*	*0.027*	*0.0016*	*0.0016*	*3.58*	*6.5*	*3.84*	*0.001*
Ho	*0.93*	*4.47*	*bd*	*0.043*	*bd*	*bd*	*0.75*	*1.20*	*0.78*	*0.011*
Er	*2.40*	*12.2*	*bd*	*0.18*	*bd*	*bd*	*1.86*	*2.83*	*1.94*	*0.057*
Tm	*0.30*	*1.71*	*bd*	*0.13*	*bd*	*bd*	*0.096*	*0.20*	*0.20*	*0.047*
Yb	*2.16*	*11.3*	*bd*	*0.16*	*bd*	*bd*	*1.65*	*2.21*	*1.65*	*0.046*
Lu	*0.33*	*1.72*	*0.0050*	*0.0047*	*bd*	*bd*	*0.28*	*0.36*	*0.26*	*0.001*
Hf	0.050	0.18	0.010	0.0068	0.0022	0.0032	0.055	0.074	0.054	0.000
Ta	0.0099	0.042	0.0010	0.0032	0.0009	0.0054	0.012	0.015	0.0091	0.000
W	0.064	0.13	0.014	0.059	0.45	2.69	0.050	0.063	0.054	0.013
Re	0.071	0.029	0.0050	0.0012	0.013	0.012	0.11	0.22	0.14	0.0002
Tl	0.12	0.21	0.16	0.061	0.80	1.84	0.36	0.035	0.077	0.0023
Pb	0.55	0.70	347	0.89	bd	bd	2.29	0.69	0.70	0.11
Bi	0.0060	0.011	0.042	0.012	bd	bd	0.0094	0.014	0.012	0.0023
Th	0.080	1.31	0.017	0.012	0.0015	0.0010	0.040	0.021	0.031	0.0008
U	0.050	0.56	0.18	0.074	0.039	0.032	0.092	0.081	0.067	0.0009

Re in waters and rock samples was determined by "kinetic" method (voltammetry, Borisova and Speranskaya, 1994). The water samples were analyzed for their oxygen and hydrogen isotopic composition, using LGR (Los Gatos) IR spectrometer. The isotope ratios are expressed in permil vs V-SMOW. The uncertainties are $\pm 0.2‰$ for $\delta^{18}O$ and $\pm 1‰$ for δD (one standard deviation).

Analytical and isotopic data for fumaroles F1 and F2 and for one gas sample from Zakatnye springs are taken from Taran (1992) and Rozhkov and Verkhovsky (1990), respectively.

The stream flow rate was measured after choosing an appropriate gauging-station site by the float method with two cross-sections of the measured depth (e.g., Rantz et al., 1982). For the Kraterny Creek

with a relatively high flow rate near the mouth, it was difficult to find a straight path with a long enough travel time. In our case, it was ~10 s. We estimate the accuracy of the flow rate determination for the Kraterny stream as ~20% using 5 independent flow rate measurements

4. Results and discussion

4.1. Gas geochemistry and geothermometry

Two samples of volcanic gas were collected from fumarole F5 with temperature of 480 °C. Two other samples were taken in 1987 by one of the authors (YT) from fumaroles F1 and F2 (Fig. 1d) with
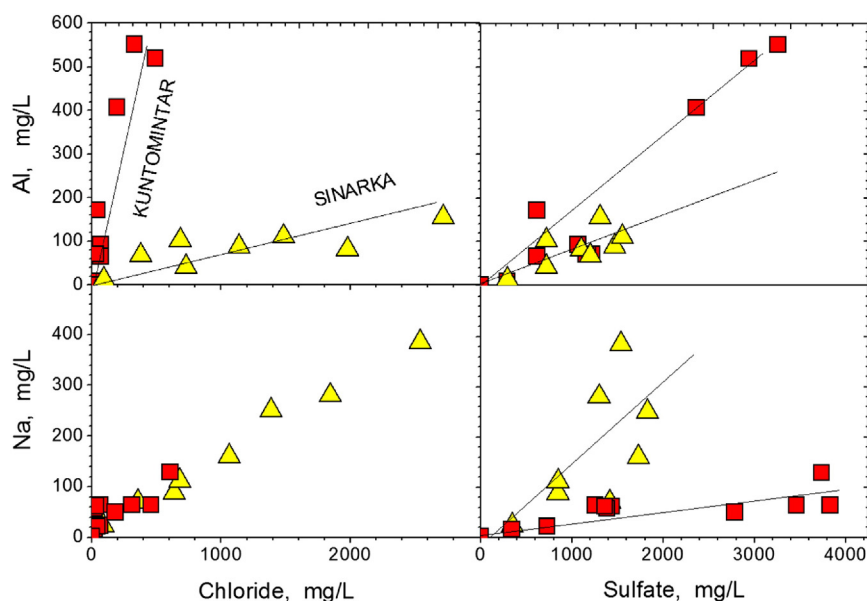
Fig. 7. Plots discriminating acidic thermal waters of Kuntamintar and Sinarka volcanoes. Symbols as in Fig. 5. See text for details.

compositions published in Taran (1992). Hot gas from the F5 fumarole (Table 2) is more water-rich than gases from F1 and F2, with low H_2 but measureable CO content. The F5 fumarole is also characterized by a higher C/S ratio (~5 vs ~3 in 1987) and about the same HCl as the lower temperature fumaroles sampled in 1987. All gases were contaminated by air: dry gases contained from 1 to 3.5 vol% of O_2, their compositions in Table 1 are corrected for air using $N_{2,c} = N_{2,m}{-}3.74O_2$ and $Ar_c = Ar_m{-}O_2/22.4$, where indices c and m refer to corrected and measured concentrations. A relatively high concentration of air was the reason for relatively low measured $^3He/^4He$ ratios for F1 and F2 fumaroles and Zakatnye bubbling gas (it had in 1987 and in 2011 almost the same O_2 concentrations, ca. 3.5 vol%). The best indicator of air contamination, He/Ne ratio, was low: in three samples, it was between 0.8 and 1.4 (air ratio is ~0.29). For the F1 gas, the corrected $^3He/^4He$ ratio of 6.4 R_a (where $R_a = 1.4 \times 10^{-6}$, the air ratio) is in the range typical for arc volcanic gases (Hilton et al., 2002). The very large difference between N2/He ratios for F1 and F2 fumaroles most probably is the result of different air contamination and can be an artifact of the air correction. Carbon isotopes in CO_2 are enriched in light isotope compared to most arc-related volcanic gases; however, such values have been reported for other arc volcanic gases (see e.g., Sano and Marty, 1995; Giggenbach, 1996). One of the explanations for the isotopically light CO_2 can be a significant contribution of carbon from the subducted sediments, taking into account that in this part of the Kamchatka-Kuril arc, the subducting old Pacific Plate has a thickness of oceanic sediments of 400–500 m (Taran, 2009 and references therein). The isotopic composition of the volcanic gas condensate collected in 2011 is similar to the condensates sampled in 1987 (Table 2). Following Sano and Marty (1995), we can estimate relative contributions to the Kuntimintar gas from the main subduction-related sources of volatiles: mantle (M), organic-rich (S) sediments and carbonates (L) of the slab (and/or underlying crust). Results are shown in Table 3. For the endmember values we accepted $R_M = 8Ra$, $\delta^{13}C_S = -25‰$ and $\delta^{13}C_L = 0‰$. Low N_2/Ar ratios, near the air values (Table 3) indicate that gases, even after correction for air, still had a large proportion of air with a part of the oxygen consumed by oxidation. The $CO_2/^3He$ and $Cl/^3He$ are within their ranges reported for volcanic gases of Kamchatka and Kuril Islands by Taran (2009).

The compositions of F5 fumarole (H_2O-H_2-CO-CO_2) gives equilibrium temperatures 590 and 620 °C (using thermodynamic data of Giggenbach, 1987), higher that the measured temperature of 480 °C. For bubbling gas of the Zakatnye springs we can estimate the CO_2 temperature assuming equilibrium in the liquid phase and using method of Taran (2005) for calculating the gas/water ratio from Ar concentration. For two gas analyses we have for $log(x_{CO2})$ in mole/kg, -2.42 and -2.34, respectively. Using the empirical CO_2 geothermometer of Taran (1988): $log(x_{CO2}) = 5.94{-}4096/T$ (liquid phase, concentration in mole/kg), the equilibrium CO_2 temperature for the Zakatnye springs is in the range of 210–220 °C.

4.2. Water chemistry

4.2.1. Water isotopes

Water isotopic composition of all collected waters including volcanic gas condensates is shown on the δD vs $\delta^{18}O$ plot (Fig. 4). Two trends can be seen. For the coastal springs the trend is apparently a mixing line between meteoric and sea water. For the acidic Cl-SO_4 waters discharging within thermal fields on volcano slopes there is a clear mixing trend between meteoric water and "andesitic" or "arc magmatic water" as defined by Taran et al. (1989) and Giggenbach (1992). Points for fumaroles are also plotted close to this mixing line. Two plots added to Fig. 4 are in agreement with the above observation: waters of coastal springs are plotted on the seawater-meteoric water δD vs Cl mixing line, whereas points for volcanic acid waters lie close to the magmatic-meteoric mixing line. The magmatic-meteoric δD vs Cl mixing line is built with the magmatic endmember having δD = $-20‰$ and Cl > 10,000 ppm (which corresponds to ~0.5 mol% of HCl). Points for SH-18 and SH-22 springs lie slightly above this mixing line indicating that probably more than simple mixing is responsible for the observed isotopic and chemical compositions of acidic waters. Fractionation at boiling and loss of steam, as well as water–rock O-shift also cannot be excluded.

4.2.2. Major elements and seawater indicators (Br, B, Sr)

Our own and literature analyses of major components of waters of the island are shown in Table 4. Acidic waters are of the SO_4-Cl type with a significantly lower Cl content and higher SO_4 content in Kuntomintar waters than those of Sinarka (Fig. 5, Table 4). It can be seen that on the SO_4 vs Cl plot (Fig. 5) all three groups of springs are well separated, and the coastal springs demonstrate a SO_4/Cl ratio close to that of seawater. Thus, the three groups show distinct main sources: seawater for the coastal springs and composition ally different magmatic sources for volcanic waters. This can also be seen in Fig. 6 (a–c) where other hydrochemical indicators: Cl/Br, Ca/Sr and Cl/B are
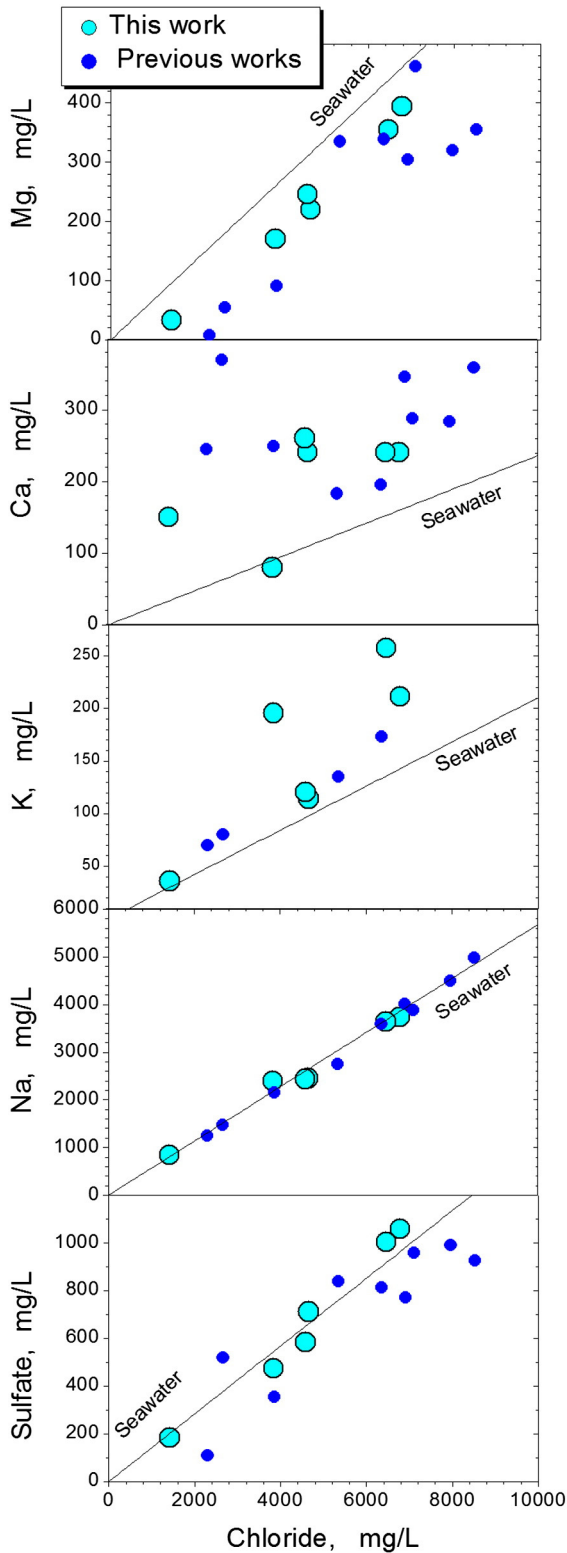
Fig. 8. Cations and sulfate vs chloride for coastal springs of Shiashkotan. There is a perfect correlation between Na and Cl, a good one for SO_4 and Cl, also a good correlation between Mg and Cl but with a deficit of Mg comparing to seawater. Both Ca and K are in excess comparing to seawater.

used. Concentrations of Br and Sr are taken from Table 5, where our data on trace elements are shown, including REE. On the Ca vs Sr plot (Fig. 6a) points for acidic volcanic water show almost no correlation between Ca and Sr, but points for coastal springs are plotted close to

the seawater line with some excess in Ca. The Cl/Br and Cl/B weight ratios for volcanic waters are close to the magmatic values reported for high-temperature gases of Kudryavy volcano (~1400 and 360, respectively, Taran et al., 1995). In the coastal springs Cl/B ratios are intermediate between magmatic and seawater values (Fig. 6b), however, Cl/Br points for the coastal springs lie close to the seawater line (Fig. 6c). Volcanic waters contain different concentrations of chloride—lower for Kuntomintar and higher for Sinarka—but show similar ratios Cl/Br and Cl/B. Difference between volcanic acid waters can be also seen in Fig. 7 where Na and Al are plotted versus Cl and SO_4. The Na vs Cl plot shows only difference in the Na and Cl concentrations for two groups but the correlation line is the same for both groups. However, Na and Al correlations with SO_4 as well as Al with Cl clearly show different endmember mixing for Sinarka and Kuntomintar acidic waters.

Volcanic acidic waters have anions loaded from volcanic gases and cations from the rock dissolution. The salinity of the coastal springs is provided by both seawater and rock dissolution. The problem with the coastal springs is what is the hot endmember? It can be infiltrated seawater heated within the volcanic edifices then mixed with cold ground water, or it can be infiltrated hot ground (meteoric) water mixed with cold seawater. Potassium, calcium and SiO_2 in the coastal springs are clearly taken up from the rock (Fig. 8)—their concentrations are above the seawater-fresh water mixing line. Magnesium shows a good correlation with chloride but with concentrations below, for some 100 mg/L, the seawater line. The intersect of ~1000 mg/L of chloride might be associated with a Mg-free hot endmember, but in that case, waters with a higher Cl content should be cooler, which is not the case. The chloride vs temperature plot (Fig. 9a) for the coastal springs is rather complicated and does not show one unambiguous trend. Only points for Zakatnye + Vodopadnye springs show a good Cl-temperature correlation that may indicate a hot endmember with a composition close to the highest-temperature Vodopadnye water. However, high Mg concentration is in contradiction with this suggestion. One of the mechanisms partially explaining high Mg concentration in a hot endmember can be the water–rock interaction with a high seawater/rock ratio at moderate temperature (<200 °C, see e.g., Taran et al., 1993; Grichuk, 1988).

In contrast to the coastal springs, volcanic waters show a good chloride-temperature correlation (Fig. 9b), suggesting the existence of a hot endmember of magmatic origin (volcanic gas condensate) with a high Cl concentration and a shallow mixing of groundwater with volcanic gases.

4.3. Geothermometry

We use a log–log plot (Fig. 10) instead of the triangle for the Na-K-Mg geothermometry of thermal waters of Shiashkotan (Giggenbach, 1988; Taran et al., 1998). Points for coastal springs are plotted within the area of partial equilibrium, whereas all acidic waters are plotted close to the average for the Shiashkotan rock (Avdeiko et al., 1991). Except for one point, Na/K ratios for the coastal springs are slightly lower than that for seawater (~29), indicating some re-equilibration. The coastal thermal waters are characterized also by relatively high SiO_2 content, which broadly correlates with the spring temperature (Fig. 11a) well below the amorphous SiO_2 curve. In contrast, acid volcanic waters show SiO_2 concentrations plotted close to the amorphous silica curve, indicating their relatively shallow formation (Fig. 11b).

For the SH16 sample (Vodopadnye springs), we calculated the temperature dependence of saturation indices for some silicate minerals and anhydrite using SOLVEQ computer code by Reed and Spycher (1984) using Al concentration from the trace element Table 5 (Fig. 12). Almost an ideal conversion to temperature near 180 °C for microcline, albite and muscovite (as proxies of much more complicated hydrothermal mineralogy in near neutral environment) may indicate the existence of an aquifer with a propylitic alteration within the island. It could be a peripheral aquifer in some way protected from the direct
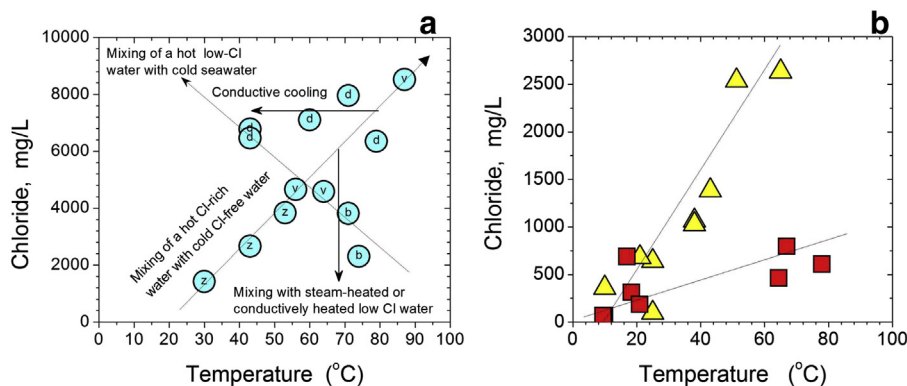
Fig. 9. Chloride vs temperature plot showing complex mixing-cooling processes for coastal springs (a) and a simple positive correlation for volcanic waters (b). Labels for coastal springs: b—Bashmachnye; d—Drobnye; v—Vodopadnye; Z—Zakatnye. See text for more details.

volcanic gas emanations, similar to bicarbonate-enriched waters at peripheries of active volcano-hydrothermal systems (e.g., Giggenbach et al., 1990), but fed mainly by seawater. Note that for anhydrite, the saturation temperature is slightly lower (ca. 150 °C).

There are several examples of a similar coastal hydrothermal activity. Sakamoto spring at the tidal zone of Satsuma Iwodjima volcano, Ryukyu Islands (Shinohara et al., 1993), is almost identical to Zakatnye springs in chemical composition and temperature. Two groups of warm springs discharge a mixture of sea- and freshwater at the coast of Socorro volcanic Island, Mexico (Taran et al., 2010). Near-neutral thermal well waters of Vulcano Island (Aiuppa et al., 2000; Cortecci and Boschetti, 2001) are significantly altered by interaction with magmatic fluids and rocks. Capasso et al. (2005) reported the compositions of shallow well waters at Stromboli Island. Some of these thermal waters (temperatures up to 47 °C) are very close in composition of major components to the coastal springs of Shiashkotan. Coastal thermal waters of Ischia (Inguaggiato et al., 2000) and Pantelleria (Parello et al., 2000), two Mediterranean volcanic islands similar in size and elevations to Shiashakotan island, demonstrate a clear 3-endmember mixing on the Cl vs temperature plots (cold seawater + Cl-free cold ground water + hot mixed water). Chiodini et al. (1996) reported the composition and geothermometry of the coastal springs at Monserrat Island (Lesser Antilles) and estimated a hot endmember (~250 °C) with chloride content higher than that of seawater (~25 g/L).

Fig. 10. Na-K-Mg systematics of thermal waters of Shiashkotan. SW—seawater.

Because the SiO_2 content of acidic volcanic waters seems to be controlled by the shallow equilibrium with amorphous silica, the saturation indices for aluminosilicate minerals for these waters do not make much sense. For the compositions of SH18 (Sinarka) and SH8 (Kuntomintar), we calculated the saturation indices for non-silicate minerals. It is seen from Fig. 13 that both Sinarka and Kuntomintar waters show saturation with respect to alunite, anhydrite, diaspore and gibbsite close to the sampling temperature between 50 °C and 100 °C. Taking into account that these springs are down-going, descending, this may indicate that beneath both volcanoes there is no deep aquifers with acid Cl-SO4 waters, and their formation is quite shallow, within the phreatic level where mixing between volcanic gases and ground waters occurs.

4.4. Trace elements

Trace elements including REE in waters and streambed sediments are shown in Tables 5 and 6. For comparing trace element patterns between Sinarka and Kuntomintar waters, we use "enrichment" coefficients normalized by titanium as a less mobile element analyzed in both waters and rock samples: $E_i = (C_i/Ti)_w/(C_i/Ti)_r$, where subscripts w and r relate to water and rock, respectively (see also Aiuppa et al., 2000 for the Ti choice). The Kuntomintar hottest spring water SH8 is compared with the corresponding sediment sample RK, and the hottest Sinarka spring SH18 is compared with the SR composition (Fig. 14). There is a similar general descending trend for both volcanoes, but due to more than one order of magnitude higher Ti concentration in the Kuntomintar sample SH8 (Table 5), the enrichment of almost all elements in the Sinarka water is approximately one log-unit higher. Note that the E_{Fe} values for both waters are equal. Sinarka water is significantly depleted in V and enriched in Cu, Pb and Re comparing to Kuntomintar water.

The log–log plots of concentrations of trace elements are shown in Fig. 15. We compare the coastal Vodopadnye springs (SH16) with seawater (Fig. 15a), Vodopadnye (SH16) with acidic Sinarka spring SH18 (Fig. 15b) and two acidic waters, Sinarka (SH18) and Kuntomintar (SH8), in Fig. 15c. Different symbols correspond to three main types of elements: chalcophile, siderophile and lithophile. Seawater concentrations are taken from Li (1991). On the coastal vs seawater plot, there are several element points plotted close to the 1:1 line: Br, Sr, Mo, V, Cd, Re, Hf. However, the most of element concentrations are up to orders of magnitude higher in the coastal thermal water than those in seawater, indicating the uptake from the rock matrix. The coastal-volcanic water comparison (Fig. 15b) reveals the enrichment of acidic water in siderophile elements, Al and some of the heavy lithophile elements. There is no correlation between chalcophile elements for neutral and acidic waters. Finally, there is a good correlation between trace elements for two acidic waters from Sinarka and
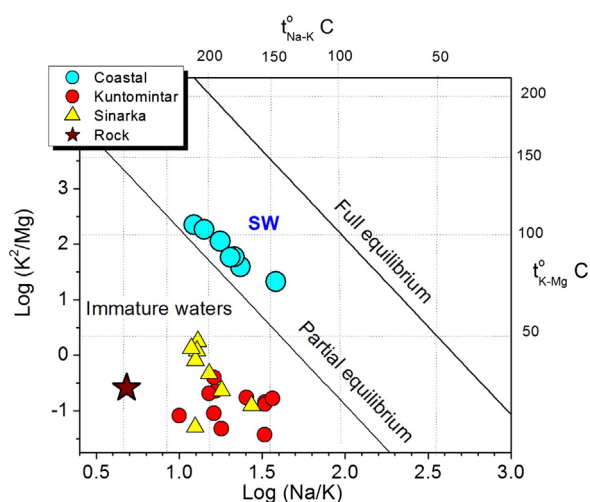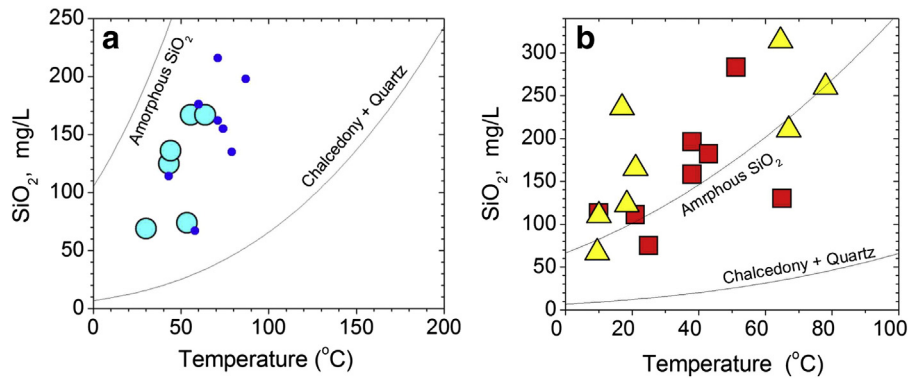
Fig. 11. SiO_2 concentration vs spring temperature. (a) for the coastal springs; (b) for volcanic acid waters. Amorphous SiO_2 solubility curve is from Fournier and Truesdell (1974). The Chalcedony + Quartz solubility line is from Giggenbach (1991).

Kuntomintar (Fig. 15c). The overall enrichment in trace elements of the Kuntomintar water comparing to Sinarka can be associated with a lower pH (2.3 vs 2.7).

4.5. Rare earth elements

The total REE concentration in the streambed sediments is surprisingly low, one to one and a half orders of magnitude lower than altered rocks of active crater facies both silicic and advanced argillic (e.g., Fulignati et al., 1999).

REE patterns normalized by chondrite (Anders and Grevesse, 1989) for sediments and acidic waters of Kuntomintar and Sinarka are shown in Fig. 16. The pattern for sediments is practically flat with a small Eu-negative anomaly. The REE distribution for waters has unusual shape with depletion in both LREE and HREE and a small Eu minimum. Similar distributions have been reported for some acidic crater lakes (Takano et al., 2004) with highly altered country rocks and by Sanada et al. (2006) in acidic waters of Tamagawa hot springs in Japan. Waters from both volcanoes cannot be distinguished using these plots. The almost one order of magnitude higher concentrations of REE for the hot Kuntomintar spring SH8 can be related to the higher Al + Fe content for this spring water and a lower pH (see above). In addition, SH8 spring is different from other Shiashkotan springs only in terms of its Al and Fe (and Ti) concentrations, which in turn are positively correlated with the spring salinities, i.e., concentrations of Cl and SO_4 (Fig. 7). The positive correlation between total REE concentration and Al + Fe has been shown by Kikawada et al. (1993) in acid waters of the Kisatsu-Shirane

area in Japan. We have a similar correlation for acid waters from both volcanoes and the coastal springs. Our points fall near the same trend on the log–log plot of the total REE vs Fe + Al (Fig. 17) as the Japanese acid waters and as all analyzed thermal waters of El Chichon volcano, Mexico (Peiffer et al., 2011).

4.6. Solute discharge and chemical erosion

There are two main solute drainages to the ocean and the Sea of Okhotsk from the island. One is the surface water flow by numerous small rivers and streams whose chemical composition can be represented by the Makarovsky stream (Table 4) with the total flow rate of all cold waters that can be estimated at ~4.9 m³/s, i.e., equal to the total precipitation input (see above). Infiltrated water is partially or totally heated within both volcano edifices and represents the hydrothermal
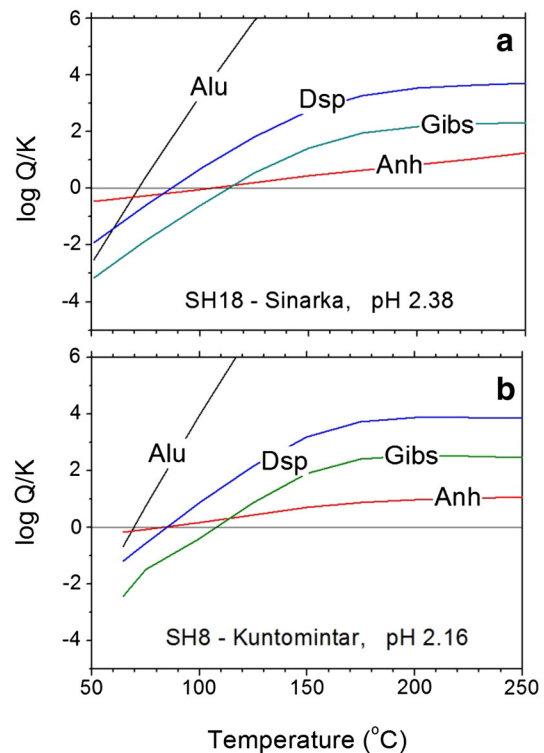

Fig. 13. Saturation indices vs temperature for non-silicate minerals for volcanic acid waters of Sinarka and Kuntomintar volcanoes. See text for discussion. Alu—alunite; Dsp—diaspore; Gibs—gibbsite; Ahn—anhydrite.

Fig. 12. Saturation indices vs temperature for the composition of the Vodopadnye coastal spring, sample SH16. Mcl—microcline; Alb—albite; Qtz—quartz; Anh—anhydrite.

Table 6
Trace elements in streambed sediments (enriched in Fe-oxides) from thermal fields of Kuntomintar and Sinarka collected in the vicinity of acid springs SH8 (Kuntomintar) and SH18 (Sinarka) (concentrations in ppm). Concentrations of REE are highlighted by italic font.

Element	RK	RS
Be	0.067	0.146
Ti	2093	1698
V	62	102
Cr	0.23	1.49
Mn	67.6	465
Fe	19959	114277
Co	2.4	8.02
Ni	0.17	1.6
Cu	7.63	24.6
Zn	10.6	32.1
Se	2.59	1.23
Rb	0.708	3.67
Sr	95.4	68.5
Y	4.26	6.31
Zr	20.7	26.8
Nb	2.27	0.406
Mo	1.11	2.04
Cd	0.021	0.041
Sn	0.804	0.946
Sb	2.28	0.38
Cs	0.082	0.66
Ba	38	78.1
La	*0.824*	*1.08*
Ce	*2.03*	*3.16*
Pr	*0.292*	*0.464*
Nd	*1.32*	*2.38*
Sm	*0.397*	*0.744*
Eu	*0.12*	*0.207*
Gd	*0.48*	*0.989*
Tb	*0.094*	*0.18*
Dy	*0.74*	*1.23*
Ho	*0.144*	*0.276*
Er	*0.515*	*0.881*
Tm	*0.075*	*0.133*
Yb	*0.509*	*0.927*
Lu	*0.081*	*0.148*
Hf	0.655	0.883
Ta	5.12	0.044
Re	0.505	<0,002
Tl	0.171	0.113
Pb	8.87	5.73
Bi	0.15	0.252
Th	0.21	0.358
U	0.292	0.319
Re	0.704	0.014

that they transport to the Pacific Ocean about 1 g/s of Cl and 2.7 g/s of sulfur. Therefore, the volcano-hydrothermal output of chlorine and sulfur can be estimated at $359 \times 0.5 + 67 \times 0.5 + 1 = 214$ g/s of Cl and $1/3(1625 \times 0.5 + 730 \times 0.5 + 2.7) = 393$ g/s of S. Taking into account the accuracy of not less than 20%, we can say that Shiashkotan volcanoes through their hydrothermal systems emit some 20 ± 5 t/day of Cl and 35 ± 7 t/day of S. These values are rather high and within the range of the measured hydrothermal outputs from other volcanoes. Rowe et al. (1995) have estimated 38 t/d of Cl and 30 t/d of S in the main acid drainage of Poás volcano, Costa Rica. Taran and Peiffer (2009) have estimated the hydrothermal Cl flux from El Chichon volcano as 470 g/s or ~ 42 t/day. Lassen Peak springs (Sorey, 1986) emit ~40 g/s of Cl or only ~4 t/d (see Taran and Peiffer, 2009 and Chiodini et al., 2014 for more examples).

The cation output plus SiO_2 is a measure of chemical erosion (e.g., Rad et al., 2007 and references therein). It is not clear how to estimate the chemical weathering by the coastal springs of Shiashkotan. They have a high mineralization, and their total discharge was estimated by Markhinin and Stratula as ~50 l/s. However, the main contributor of their salinity, as shown above (Figs. 3 and 7), is seawater. The part of their mineralization due to water–rock interaction can be estimated as the excess of SiO_2 and cations compared with seawater. In any case, the contribution of coastal springs is low compared to the acid drainage flux.

The chemistry of the Makarovsky stream is shown in Table 3. The source of this stream, as mentioned above, is perennial snow of the Makarov isthmus. A relatively high Cl content (14 to 25 mg/kg) is most probably related to the oceanic water aerosol in rain water (see the rain water analyses in Table 2). The total dissolved cation + SiO_2 content of the stream water ranges from 31 to 60 mg/kg. Taking 45 mg/L as an average cation concentration in surface waters of the island and assuming, following Rad et al. (2007), that half has marine origin, we can estimate the surface chemical weathering rate with ~4.9 m^3/s of the surface + subsurface flow from 118 km^2 of the island area as 27 ton/km^2/year with an error probably close to 50%.

The minimum value of the chemical erosion by thermal acidic waters from both volcano-hydrothermal systems can be estimated using the flow rates of the two acid streams, Kraterny and Agglomeratovy. It gives ~140 ton/km^2/year, 5 times higher than the surface flux. These values can be compared with the chemical erosion estimations for tropical volcanic islands Guadeloupe (Lesser Antilles) and Reunion by Rad et al. (2007). The comparison is shown in Table 7. Since the annual
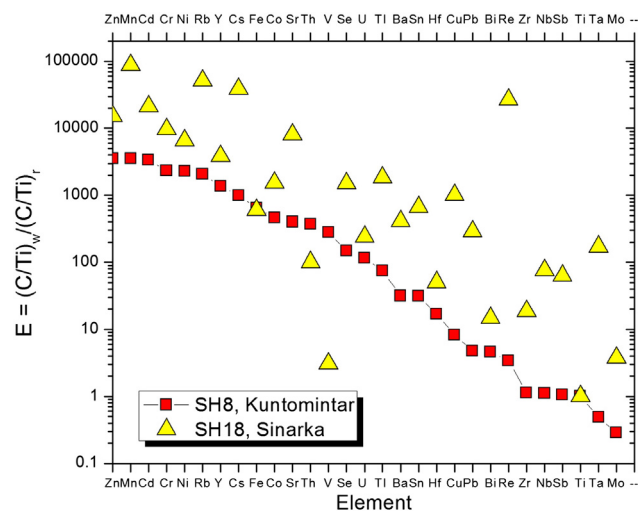
outflow. For Shiashkotan, there are three main volcano-hydrothermal drainages. Kuntomintar thermal fields are drained by Kraterny Creek into the Sea of Okhotsk. The Sinarka thermal fields are drained to the Severgina strait by the Agglomeratovy river. The NE thermal field of Sinarka is drained by the Sernaya (Sulfur) river to the Pacific Ocean. Both the Kraterny Creek and the Agglomeratovy river are acid (Table 4) and produce a considerable discolored zones in the sea in the vicinity of their mouths indicating a high Al content of the stream water (Fig. 1b). The measured total discharge of the Kraterny close to the mouth is 500 ± 100 l/s, and it contains 67 mg/L of chloride and 730 mg/L of sulfate. For the Agglomeratovy stream, Markhinin and Stratula (1977) reported about 2 m^3/s of the water flow with 357 ppm of Cl and 1625 ppm of SO_4 in 1964. It seems this flow rate value was over-estimated. We did not measure the Agglomeratovy river discharge rate at the mouth but visually it is very similar to the Kraterny Creek mouth and therefore we accept for the Agglomeratovy river the same value of 500 ± 100 l/s. There are no data for the Sernaya River flow rate and chemical composition, but the near-neutral hot pools-springs of the NE field of Sinarka have the measured discharge rates at about 20 l/s in total (Stratula, 1969) with an average chloride ~50 mg/L and sulfate ~400 mg/L (Zharkov et al., 2011), which means

Fig. 14. Enrichment coefficients for acid volcanic waters of Kuntomintar and Sinarka normalized by titanium relative corresponding streambed sediments enriched in Fe-oxides. Descending order for the SH8 Kuntomintar sample. The total REE enrichment is not shown. It is very close to yttrium values.
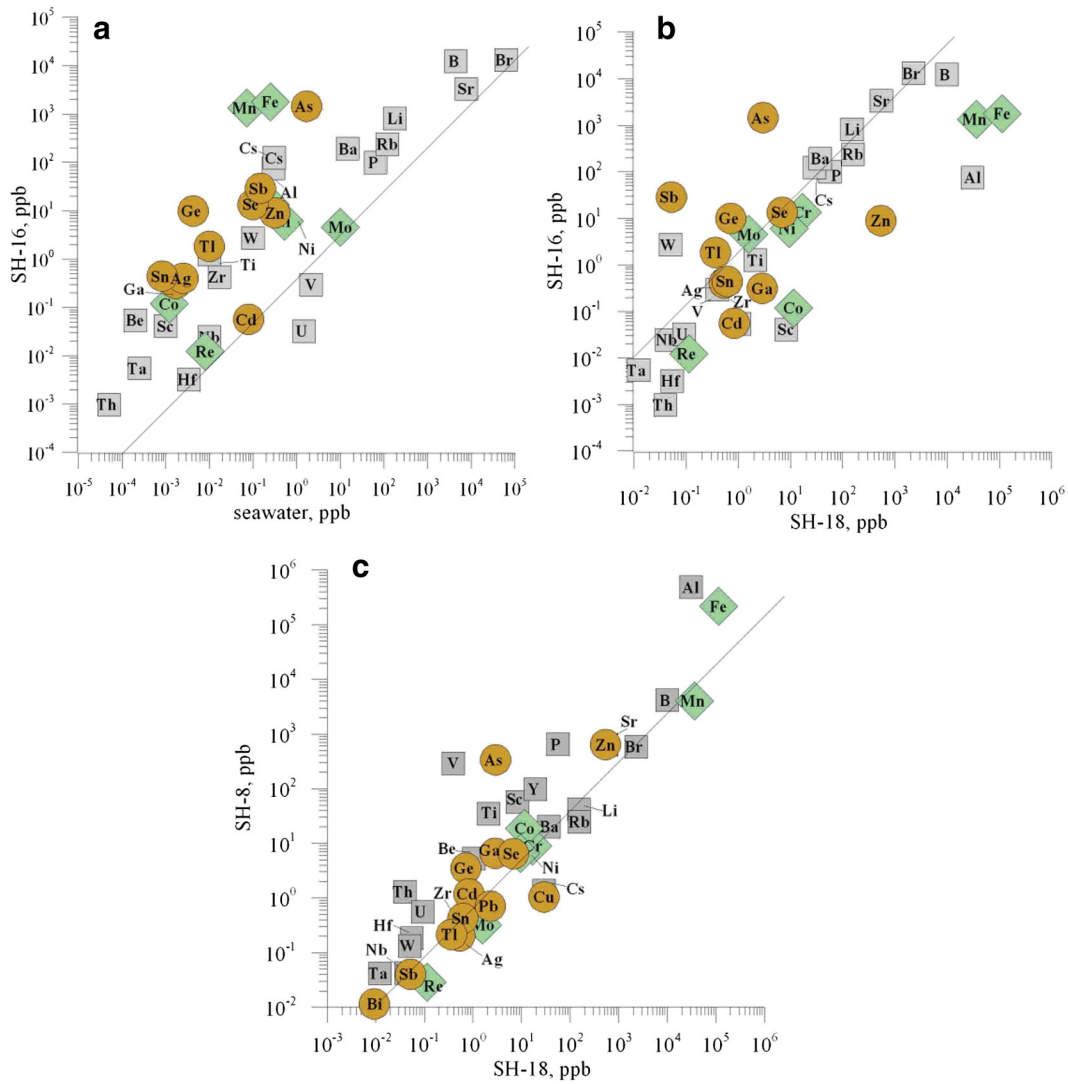
Fig. 15. Comparative log–log plots for concentrations of trace elements in Shiashkotan thermal waters. (a) Coastal Vodopadny spring (SH16) vs seawater (from Li, 1991); (b) Vodopadny spring vs acidic SO₄-Cl Sinarka spring; (c) Acidic springs of Sinarka (SH18) and Kuntomintar (SH8). Squares—lithophile elements, diamonds—siderophile elements and circles—chalcophile elements. See text for discussion.

precipitation rate is 3.5 times lower and the annual temperature is low, the surface flux by cold waters for Shiashkotan is 3–4 times smaller than that of the tropical islands. The subsurface (hydrothermal) fluxes at Shiashkotan are about two times lower, but as it was mentioned above, this is a minimum estimation made for two main hydrothermal drainage of the island. In any case, for the hydrothermal weathering,
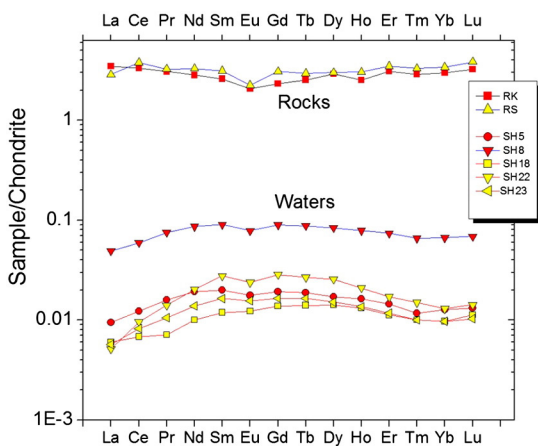
Fig. 16. REE patterns for the streambed sediments and acidic volcanic waters of Kuntomintar (dark symbols) and Sinarka (light symbols). See text for more details.
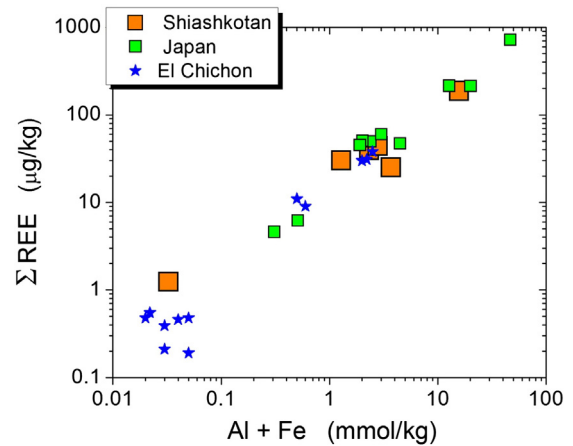
Fig. 17. Total REE vs Al + Fe. Comparison with data by Kikawada et al. (1993) for acid waters of the Kisatsu-Shirane region and Peiffer et al. (2011) for El Chichon volcano-hydrothermal system.

Table 7
Chemical weathering rates for Shiashkotan Island comparing with tropical volcanic islands (after Rad et al., 2007). Data for Shiashkotan are highlighted by the bold font.

Island	Shiashkotan	Guadeloupe	Reunion
Surface area, km^2	**118**	1080	2500
Annual precipitation, mm	**1300**	5000	4500
Mean annual temperature (°C)	**4**	28	23
Chemical erosion, ton/km^2/year			
Surface	**27**	140	100
Subsurface	**140**	290	270
Total	**167**	430	370

there is an interplay between at least two main parameters: the total infiltration water flow and the salinity (acidity) of the hydrothermal water.

5. Conclusions

A small volcanic island Shiashkotan at the Northern Kuril chain is characterized by strong volcanic gas emissions with temperature of fumaroles >450 °C and variable and strong hydrothermal activity that includes the discharge of acidic SO$_4$-Cl waters at the slopes of two volcanoes composing the island, Sinarka and Kuntomintar, as well as hot near-neutral saline coastal springs on the Sea of Okhotsk shore line.

Volcanic gas from Kuntomintar is a typical arc-type gas with the corrected ^{3}He/^{4}He of 6.4Ra, δ^{13}C-CO$_2$ in the −8‰ to −10‰ range and volcanic vapors containing near a half of the "arc-type" water.

Acidic volcanic waters of the two volcanoes, although similar in pH, are different in their Cl/SO$_4$, Al + Fe and the total REE concentrations. Their water isotopic compositions correspond to mixing of meteoric water with volcanic vapor. In contrast, all coastal springs show a single pattern of mixing of meteoric and marine water in both chemical and water isotopic composition.

Estimations of deep temperatures using saturation indices reveal a shallow formation for the acid volcanic waters (50–100 °C) and a good conversion to the equilibrium temperature of ~180 °C for the coastal springs.

Kuntamintar and Sinarka volcanoes are also characterized by different trace element concentrations in their acidic waters and their Ti-normalized enrichment factors relative to the streambed sediments. The chondrite-normalized REE patterns for acidic waters are not distinguishable for both volcanoes. They have an unusual shape with a slight depletion in both LREE and HREE and a small Eu minimum. The total REE concentration for both volcanic waters is proportional to the Al + Fe concentration with a slope that seems to be universal for acidic SO$_4$-Cl volcanic waters everywhere.

The measured volcano-hydrothermal outputs of Cl and S by acidic waters from Shiashkotan are 20 ± 5 and 35 ± 7 t/day, respectively, with the Sinarka flux about 5 times higher than the flux from Kuntomintar.

The chemical weathering rates (chemical erosion) for the surface (cold) and subsurface (hydrothermal) outflows for Shiashkotan are roughly estimated at 27 and 140 ton/km^2/year. The surface effect is 3–4 times smaller than that for tropical volcanic islands (Guadeloupe and Reunion) and is proportional to the annual precipitation rate. The estimated subsurface (hydrothermal) weathering for Shiashkotan is about two times lower than the corresponding values for tropical islands.

References

Aiuppa, A., Dongarra, G., Capasso, G., Allard, P., 2000. Trace metals in the thermal waters of Vulcano Island. J. Volcanol. Geotherm. Res. 98, 189–207.

Anders, E., Grevesse, N., 1989. Abundances of the elements: meteoritic and solar. Geochim. Cosmochim. Acta 53, 197–214.

Atlas, 2007. Atlas of the Sakhalin District. FGUP DV AGP, Khabarovsk (107 pp.).

Avdeiko, G.P., Volynets, O.N., Antonov, A.Y., Tsvetkov, A.A., 1991. Kurile island-arc volcanism: structural and petrological aspects. Tectonophysics 199, 271–287.

Borisova, L.V., Speranskaya, E.F., 1994. Kinetic methods for Re determination. Nauka, Moscow (72 pp, (in Russian)).

Capasso, G., Carapezza, M.L., Federico, C., Inguaggiato, S., Rizzo, A., 2005. Geochemical variations in fluids from Stromboli volcano (Italy): early evidences of magma ascent during 2002–2003 eruption. Bull. Volcanol. 68, 118–134.

Chiodini, G., Cioni, R., Frullani, A., Guidi, M., Marini, L., Prati, F., Raco, B., 1996. Fluid geochemistry of Montserrat Island, West Indies. Bull. Volcanol. 58, 380–392.

Chiodini, G., Liccioli, C., Vaselli, O., Calabrese, S., Tassi, F., Caliro, S., D'Alessandro, W., 2014. The Domuyo volcanic system: an enormous geothermal resource in Argentine Patagonia. J. Volcanol. Geotherm. Res. 274, 71–77.

Cortecci, G., Boschetti, T., 2001. Geochemical model of the phreatic system of Vulcano (Aeolian Islands, Italy). In: Cidu (Ed.), Water-Rock Interaction 2001. Swets & Zeitlinger, Lisse, pp. 795–798.

Fournier, R.O., Truesdell, A.H., 1974. Geochemical indicators of subsurface temperature - Part 2. USGS J. Res. 2, 263–270.

Fulignati, P., Gioncada, A., Sbrana, A., 1999. Rare-earth element (REE) behaviour in the alteration facies of the active magmatic–hydrothermal system of Vulcano (Aeolian Islands, Italy). J. Volcanol. Geotherm. Res. 88, 325–342.

Giggenbach, W.F., 1987. Redox processes governing the chemistry of fumarolic gas discharges from White Island, New Zealand. Appl. Geochem. 2, 143–161.

Giggenbach, W.F., 1988. Geothermal solute equilibria. Derivation of Na–K–Mg–Ca geoindicators. Geochim. Cosmochim. Acta 52, 2749–2765.

Giggenbach, W.F., 1991. Chemical techniques in geothermal exploration. UNITAR/UNDP Handbook of Application of Geochemistry in Geothermal Reservoir Development, pp. 119–144.

Giggenbach, W.F., 1992. Isotopic shifts in waters from geothermal and volcanic systems along convergent plate boundaries and their origin. Earth Planet. Sci. Lett. 113, 495–510.

Giggenbach, W.F., 1996. Chemical composition of volcanic gases. In: Scarpa, Tilling (Eds.), Monitoring and Mitigation of Volcanic Hazards. Springer-Verlag, pp. 221–256.

Giggenbach, W.F., Goguel, R.L., 1989. Collection and analysis of geothermal and volcanic water and gas discharges. New Zealand DSIR Chem. Division Report 2407, Christchurch, New Zealand (88 pp.).

Giggenbach, W.F., Garcia, N., Londoño, C.A., Rodriguez, V.L., Rojas, G.N., Calvache, V.M.L., 1990. The chemistry of fumarolic vapor and thermal-spring discharges from the Nevado del Ruiz volcanic-magmatic hydrothermal system, Colombia. J. Volcanol. Geotherm. Res. 42, 13–39.

Gorshkov, G.S., 1970. Volcanism of the Upper Mantle: Investigations in the Kuril Island Arc. Plenum Press, NY (385 pp.).

Grichuk, D.V., 1988. Thermodynamic modeling of the chemical and isotopic composition of a hydrothermal system: Doklady. Earth Sci. 298, 1222–1225.

Hedenquist, J.W., Aoki, M., Shinohara, H., 1994. Flux of volatiles and ore-forming metals from the magmatic-hydrothermal system of Satsuma Iwojima Volcano. Geology 22, 585–588.

Inguaggiato, S., Pecoraino, G., D'Amore, F., 2000. Chemical and isotopic characterization of fluid manifestations at Ischia Island. J. Volcanol. Geotherm. Res. 99, 151–178.

Kikawada, Y., Oi, T., Honda, T., Osaka, T., Kakihana, H., 1993. Lanthanoid abundances of acidic hot spring and crater lake waters in the Kusatsu-Shirane volcano region, Japan. Geochem. J. 27, 19–33.

Li, Y.-H., 1991. Distribution patterns of the elements in the ocean: a synthesis. Geochim. Cosmochim. Acta 55, 3223–3240.

Lopez, D.L., Williams, S.N., 1993. Catastrophic volcanic collapse relation to hydrothermal processes. Science 260, 1794–1796.

Markhinin, E.K., Stratula, D.S., 1977. Hydrothermal Systems of Kuril Islands. Nauka, Moscow 227 p, (in Russian).

Parello, F., Allard, P., D'Alessandro, W., Federico, C., Jean-Baptiste, P., Catani, O., 2000. Isotope geochemistry of Pantelleria volcanic fluids. Sicily Channel rift: a mantle volatile endmember for volcanism in southern Europe. Earth Planet. Sci. Lett. 180, 325–329.

Peiffer, L., Taran, Y., Lounejeva, E., Solís-Pichardo, G., Rouwet, D., Bernard-Romero, R., 2011. Tracing thermal aquifers of El Chichón volcano-hydrothermal system (México) with ^{87}Sr/^{86}Sr, Ca/Sr and REE. J. Volcanol. Geotherm. Res. 205, 55–66.

Rad, S.D., Allègre, C.J., Louvat, P., 2007. Hidden erosion on volcanic islands. Earth Planet. Sci. Lett. 262, 109–124.

Rantz, S.E., et al., 1982. Measurement and computation of stream flow. U.S. Geol. Survey Water Supply Paper 2175. Measurement of Stage and Discharge Volume 1 (284 pp.).

Reed, M.H., Spycher, N.F., 1984. Calculation of pH and mineral equilibria in hydrothermal waters with application to geothermometry and studies of boiling and dilution. Geochim. Cosmochim. Acta 48, 1479–1492.

Reid, M.E., Sisson, T.W., Brien, D.L., 2001. Volcano collapse promoted by hydrothermal alteration and edifice shape Mount Rainier. Wash. Geol. 29, 779–782.

Rowe Jr., G.L., Brantley, S.L., Fernandez, J.F., Borgia, A., 1995. The chemical and hydrologic structure of Poás volcano, Costa Rica. J. Volcanol. Geotherm. Res. 64, 233–267.

Rozhkov, A.M., Verkhovsky, A.B., 1990. Geochemistry of Noble Gases in High Temperature Hydrothermal Systems. Nauka, Moscow 167 pp, (in Russian).

Sanada, T., Takamatsu, N., Yoshiike, Y., 2006. Geochemical interpretation of long-term variations in rare earth element concentrations in acidic hot spring waters from the Tamagawa geothermal area, Japan. Geothermics 35, 141–155.

Sano, Y., Marty, B., 1995. Origin of carbon in fumarolic gas from island arcs. Chem. Geol. 119, 265–274.

Shinohara, H., 2013. Volatile flux from subduction zone volcanoes: insights from a detailed evaluation of the fluxes from volcanoes in Japan. J. Volcanol. Geotherm. Res. 268, 46–63.

Shinohara, H., Giggenbach, W., Kazahaya, K., Hedenquist, J., 1993. Geochemistry of volcanic gases and hot springs from Satsuma-Iwojima, Japan. Geochem. J. 27, 271–285.

Sorey, M.L., 1986. Hot spring monitoring at Lassen Volcanic National Park, California, 1983-1985. Proceedings, 11th Workshop on Geothermal Reservoir Engineering. Stanford University, pp. 141–147.

Stratula, D.S., 1969. Volcanoes and hot springs of Shiashkotan Island. (PhD Thesis), Instituite of Volcanology, Petropavlovsk-Kamchatsky (in Russian).

Takano, B., Suzuki, K., Sugimori, K., Ohba, T., Fazlullin, S.M., Bernard, A., Sumarti, S., Sukhyar, R., Hirabayashi, M., 2004. Bathymetric and geochemical investigation of Kawah Ijen Crater Lake, East Java, Indonesia. J. Volcanol. Geotherm. Res. 135, 299–329.

Taran, Y.A., 1988. Geochemistry of Geothermal Gases. Nauka, Moscow, p. 170 (in Russian).

Taran, Y., 1992. Chemical and isotopic composition of fumarolic gases from Kamchatka and Kurile Islands. Rept. Geol. Surv. Japan 279, 183–186.

Taran, Y.A., 2005. A method for determination of the gas–water ratio in bubbling springs. Geophys. Res. Lett. 32, L23403. http://dx.doi.org/10.1029/2005GL024547.

Taran, Y.A., 2009. Geochemistry of volcanic and hydrothermal fluids and volatile budget of the Kamchatka–Kuril subduction zone. Geochim. Cosmochim. Acta 73, 1067–1094.

Taran, Y.A., Peiffer, L., 2009. Hydrology, hydrochemistry and geothermal potential of El Chichón volcano–hydrothermal system, Mexico. Geothermics 38, 370–378.

Taran, Y.A., Gavrilenko, G.P., Chertkova, L.V., Grichuk, D.V., 1993. A geochemical model of the Ushishir volcano-hydrothermal system, Kuril Islands. Volcanol .Seismol. 1, 64–79.

Taran, Y.A., Hedequist, J.W., Korzhinsky, M.A., Tkachenko, S.I., Shmulovich, K.I., 1995. Geochemistry of magmatic gases of Kudryavy volcano, Iturup. Kuril islands. Geochim. Cosmochim. Acta 59, 1741–1761.

Taran, Y., Fisher, T.P., Pokrovsky, B., Sano, Y., Armienta, M., Macias, J.L., 1998. Geochemistry of the volcano–hydrothermal system of El Chichón Volcano, Chiapas, Mexico. Bull. Volcanol. 59, 436–449.

Taran, Y., Inguaggiato, S., Varley, N.R., Cienfuegos, E., 2010. Geochemistry of H2 and CH4-enriched hydrothermal fluids of Socorro island, Revillagigedo archipelago. Mexico. Evidences for serpentinization and abiogenic methane. Geofluids 10, 542–555.

Wahrenberger, C., Seward, T.M., Dietrich, V., 2002. Volatile trace-element transport in high-temperature gases from Kudryavy volcano (Iturup, Kurile Islands, Russia). In: Hellmann, R., Wood, S. (Eds.), Water-rock interaction, ore deposits and environmental geochemistry. A tribute to David A. Crerar. The Geochemical Society Sp. Publication N°7, pp. 307–327.

Zharkov, R.V., Kozlov, D.N., Degterev, A.V., 2011. Current fumarolic and hydrothermal activity of Sinarka volcano, Shiashkotan, Kuril Island. Vestn. KRAUNTS 17, 179–184 (in Russian).